Available online at www.sciencedirect.com
ScienceDirect
Ceramics International 38 (2012) 909–918
CERAMICS INTERNATIONAL
www.elsevier.com/locate/ceramint

Preparation of high solid loading titania suspension in gelcasting using modified boiling rice extract (MBRE) as binder

S. Mahata [a], M.M. Nandi [b], B. Mondal [a,*]

[a] CSIR- Central Mechanical Engineering Research Institute, Centre for Advanced Material Processing, Mahatma Gandhi Avenue, Durgapur 713 209, India
[b] Dept. of Chemistry, National Institute of Technology, Durgapur, India

Received 18 May 2011; received in revised form 1 August 2011; accepted 4 August 2011
Available online 11 August 2011

Abstract

Preparation of high solid loading homogeneous titania suspension using modified boiling rice extract (BRE) as consolidator (network-former)/binder for gelcasting application has been investigated. To achieve in situ consolidation forming of TiO_2 ceramic, the gel network formed by swelling and gelatinization of the modified BRE (MBRE) with 2-hydroxyethylmethacrylate was studied. The dispersion behaviour of the titania powder and rheology of the suspension under the influence of binder content, dispersant (Darvan 821A) concentration and pH of the dispersing media have been discussed. The present process of gel casting deals with 50–80 weight% solid loading of titania particles with MBRE (2–10 weight% to that of total solid loading) in presence of dispersant (ammonium salt of polyacrylic acid [$(C_4H_5O_2–NH_4^+)n$]). The influence of BRE concentration and solid particle loading on rheological properties of aqueous titania suspensions has been analyzed under steady and oscillatory shear conditions. Thermogravimetry (TG) and differential thermal analysis (DTA) on gelcast green body has been evaluated and analyzed. The characterization of green and sintered body has been done with respect to density, porosity and microstructure.

Keywords: Gel casting; Slurry; Zeta potential; Rheology; Dispersion and sintering

1. Introduction

Gelcasting is a near net shape forming technique for making good quality intricate parts in industrial application. This is a method based on gelling of ceramic suspensions by means of in situ polymerization of water soluble monomer. Generally ceramic processing techniques including spray drying, slip casting, pressure casting, tape casting and gel casting are based on innovative concepts of handling and molding high solid loading ceramic suspensions to have a desired shape [1,2] with adequate green strength [3,4]. Among these techniques, the gelcasting process is rapidly adopted in industries due to its versatility. New gelling system without toxicity or low toxicity has been attempted by different researchers [5,6].

Besides chemical cross-linking of the monomer, physical cross-linking of some suitable polymers without toxicity such as cellulose, starch, agarose, caragenans has also been attempted earlier [7–10]. Generally, starch is a polysaccharide comprising glucose monomers joined in α-1,4 and α-1,6 glycosidic linkages. The simplest form of starch is the linear polymer amylose and branched polymer amylopectin. Boiling rice extract from indica rice contains 17–22% amylose compared to ~25% in normal starch and has high adhesive properties [11]. Starch consolidation casting using native or modified starches [12] has the prospective of maintaining high degree of homogeneity in the slurry for gelcast fabrication of various types of ceramics. The mechanism of starch consolidation casting was represented by investigators [13,14]. The modified starch swells on heating above 50 °C and finally gelatinizes ~65 °C by absorbing water and extends the molecular chains of starch molecules. Fine TiO_2 particles permeate into these molecules and subsequent rheological changes transform viscous suspension to consolidate ceramic particles. The amylose type polymer may be more responsible for gelling properties of starches. The disrupted crystalline regions of the starch granules adsorb at the surface of the ceramic particles, act like a binder and thus improve the strength of the consolidated body. The mechanism of starch consolidation casting is schematically represented in Fig. 1.

* Corresponding author. Tel.: +91 343 6510218; fax: +91 343 2546745.
E-mail addresses: bnmondal@rediffmail.com, bnmondal@cmeri.res.in (B. Mondal).

0272-8842/$36.00
doi:10.1016/j.ceramint.2011.08.010

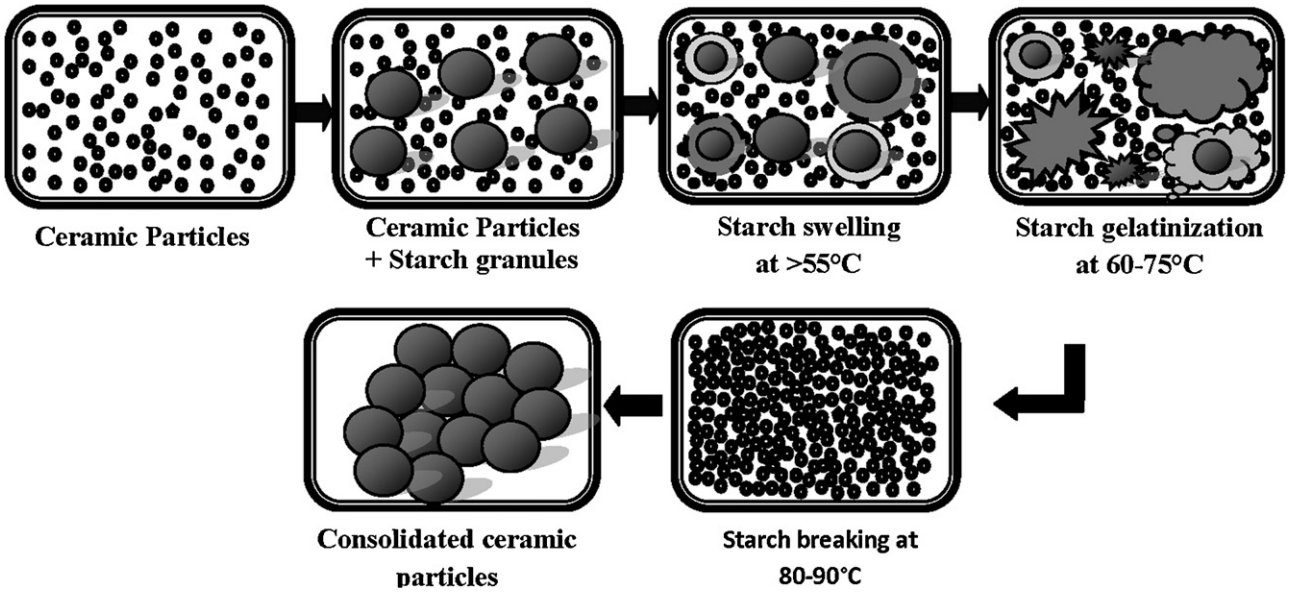

Fig. 1. Schematic view of green body formation mechanism in modified starch consolidation gelcasting.

An attempt has been made to produce gel cast of titania powders using modified boiling rice extract (BRE) (2–10 weight% to that of total solid content) as consolidator/natural binder for the fabrication of dense ceramic component. The present work deals with the effect of BRE and that of total solid particle loading as on slurry rheology and gelcasting of titania. The electro kinetic and rheological behaviour of titania suspensions have been studied by changing the concentration of dispersant and pH of the dispersing medium. It also deals with the characterization of green as well as sintered parts with respect to density, porosity and microstructure.

2. Materials and experimental procedure

2.1. Materials

A commercial grade titania powder produced by Qualigens fine chemicals with 98% purity was selected as a model ceramic powder for the preparation of suspensions in the present investigation. The average particle size of the powder was 65 nm measured by dynamic light scattering method with particle size analyser and crystallite size was 8 nm calculated by Debye–Scherrer formula from XRD analysis. Followings were the essential components of this gel casting process:

- Reactive organo monomer-monofunctional 2-Hydroxyethyl-methacrylate ($H_2C{=}C(CH_3)CH_2CH_2OH$) (HEMA) (97%, Sigma–Aldrich Chemie, Germany), 0.5 weight% to that of total solid loading.
- Newly introduced consolidator/natural binder boiling rice extract (BRE), 2–10 weight% to that of total solid loading.
- Difunctional, *N*,*N*-methylenebisacrylamide, $(C_2H_3CONH)_2CH_2$ (MBAM) (Sigma–Aldrich, China), which acts as cross-linker, 0.01 weight% to that of total solid content.
- Ammonium persulfate $(NH_4)_2S_2O_8$ (98%, A.C.S. reagent, Sigma–Aldrich Inc., USA), used as initiator, 0.01 weight% to that of total solid content.
- N,N,N′,N′-tetramethylethylenediamine (TEMED) (redistilled, 99.5%, Sigma–Aldrich, Inc., USA), as catalyst, 0.01 weight% to that of total solid content.

Materials used for amylose content determination are the same as those used by Hoover and Ratnayake [15].

2.1.1. BRE extraction and starch content determination

BRE was extracted from indica rice (IR64) purchased from Indian market. Flowchart for the extraction process is shown in Fig. 2a. Accurate determination of amylose and amylopectin content in starch is very important as it influences physico-chemical properties such as gelatinization, retrogradation, water absorption, and slurry viscosity.

To determine total starch content the following steps were carried out:

- Hydrolysis of starch into soluble branched and unbranched maltodextrins by thermostable α-amylase.
- Quantitatively hydrolysis of maltodextrins to D-glucose by amyloglucosidase (AMG).
- Total glucose content was determined from strength of the glucose solution by Fehling's test method [16].

To determine total amylose content the basic protocol takes into account the iodine affinity of amylopectin and involves the following steps:

- Defatted starch was dispersed in dimethylsulfoxide (DMSO) and the absorbance at 600 nm of the dispersed starch was determined.

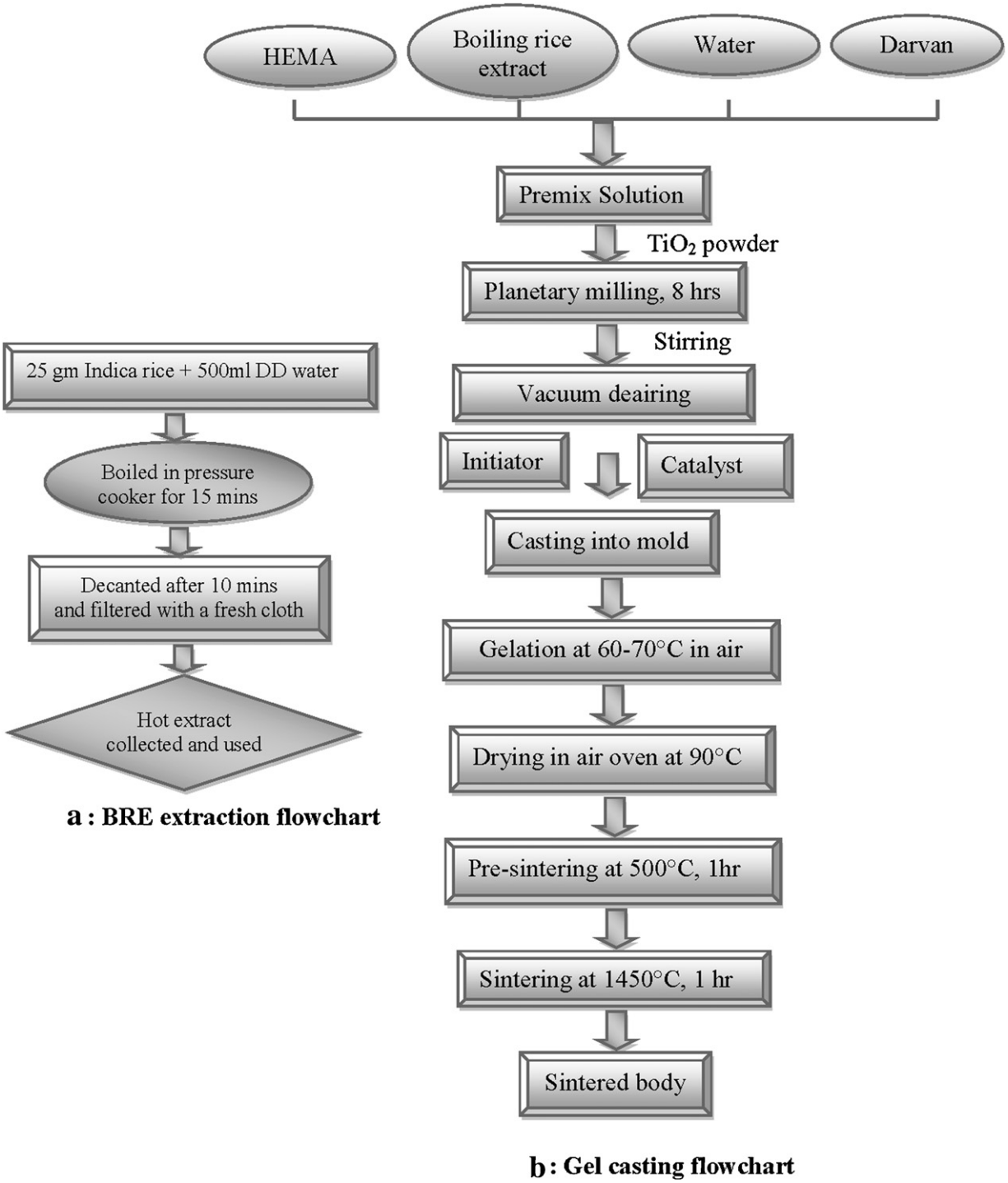

Fig. 2. (a) BRE extraction flowchart 2. (b) Gel casting flowchart.

- Total amylose content was calculated from the standard curve prepared with 0–100% amylose, using mixtures of pure amylose and amylopectin.

Total amount of amylopectin was determined from the difference of total amount of starch and amylose content. Percentages of starch, amylose and amylopectin present in the prepared BRE are 69, 21 and 48 respectively. Binding property of BRE may be attributed to the presence of these components.

2.1.2. Slurry preparation, gelcasting and characterization

The gel casting process flow chart is shown in Fig. 2b. Initially HEMA was added to BRE under stirring. It was dissolved in deionised water and Darvan 821A was added in order to obtain a premixed solution. Gel casting slurries were prepared by planetary-milling of titania powder (Pulverisette, Fritsch Industries, Germany) for 8 h in the premix solution. Aqueous suspensions were prepared separately with 50–80 weight% of solid loading. Zeta potentials and particle size were measured for 0.05 weight% diluted suspension of slurry with Malvern

Zetasizer (Particle size analyzer), Nano ZS90 apparatus (Malvern Instruments Limited, UK, and Model: ZEN 3690). The titania particles were suspended in a 0.01 M NaCl solution so that a constant electrical double layer thickness can be maintained for different ranges of solid loading.

Rheological properties of the titania suspensions with different percentages of solid loading and BRE content were measured by Visco Tech Air Bearing Fluids Rheometer with Fluid Jackets and Huber Circulator (Rheologica Instruments AB, Sweden, Model: Visco Tech CC3) with vane system which prevents the sedimentation because slurries tend to settle down or sediment during analysis. The oscillation stress sweep and strain sweep were taken for the measurement of strain amplitude with storage/loss modulus. Both the initiator, 0.01 weight% aqueous solution of ammonium persulfate and the catalyst viz. TEMED were added just before casting into a steel/aluminium mold. The premix solution undergoes free-radical-initiated polymerization in the presence of initiator, ammonium persulphate $(NH_4)_2S_2O_8$. The reaction was accelerated by the catalyst N,N,N′,N′-tetramethylenediamine (TEMED). Gelation was done at 60–70 °C in an air oven (TEST MASTER, Testing Instrument Manufacturing Company, Kolkata, India). After gelation, a variety of shaped samples was demolded and green bodies were then put into the air-oven for 48–96 h at 90 °C until constant weight was obtained.

Thermal analysis for green gelcast part of TiO_2 with different BRE percentages was performed in a simultaneous thermal analyzer (Netzsch, STA-449, Jupiter, Germany). Samples of about 60 mg were heated from 30 °C to 1550 °C at a heating rate of 10 °C/min and a flow rate of 20 mL/min in a nitrogen atmosphere. The dried green bodies were slowly heated from room temperature to 650 °C with a heating rate of 3 °C/min. The pre-sintered samples were sintered in a high temperature electric chamber furnace (Bysakh & Company, Kolkata, India Model: 70C 15) at 1450 °C for 1 h. This sintering temperature is higher than the sintering temperature of TiO_2 (1400 °C) to obtain higher dense components. Infrared quantitative analysis of HEMA, dry BRE powder and green compact were carried out with Shimadzu Fourier Transform Infrared Spectrometer (Model: IR Prestige-21, Japan).

XRD measurements were performed using a powder diffractometer (Shimadzu Model. XRD 6000, Japan) operating in the reflection mode with CuKα radiation. The patterns were recorded over the angular range of 10–75° (2θ) with a scan rate of 2.8°/min. The green and sintered densities were measured by Archimedes' method using kerosene media. Drying and sintering shrinkages were also measured. The surface microstructure of polished green and sintered (1450 °C) samples were observed by Field Emission Scanning Electron Microscope (CARL-ZEISS-SMT-LTD, Germany, Model: SUPRA40).

3. Results and discussion

3.1. Effect of modification of BRE with HEMA and its impact on gelcasting

The modification of BRE with HEMA is evidenced by Fourier transform infrared (FTIR) spectroscopy, X-ray diffraction analysis and thermal analysis as well as micro structural observations (FESEM). The networking of the polymeric changes takes place may be observed from FTIR. FTIR results indicate some modification has taken place in case of BRE with HEMA as depicted in Fig. 3.

3.2. Fourier transform infrared (FTIR) spectroscopy

Fig. 3 shows the Fourier transform infrared (FTIR) spectra of BRE powder (dried at 60 °C), HEMA, BRE with HEMA (8 weight%) and green gelcast body. The bond stretch around 937 cm^{-1} and 837 cm^{-1} are assigned to C–H bond on starch molecules. Several perceptible absorbencies in the fingerprint region, at 1156, 1083, 1023 and 937 cm^{-1}, are associated with native starch and attributed to the vibration of C–O–H deformation [17]. Absorbance in the 1000–970 cm^{-1} frequency range, are noticeable as IR spectra of amylose. Strong absorption band at 1023 cm^{-1} is probably due to the stretching of the C–OH bond [17]. Characteristic absorption bands at 1156 and 1083 cm^{-1} in the infrared spectra of BRE are both assigned as the coupling of C–O, C–C and O–H bond stretching, bending and asymmetric stretching of the C–O–C glycosidic linkage. Presence of the 1295 cm^{-1} band may be the characteristic infrared band of amylopectin complexes or regular fold conformation in amylose. The absorbance at 1350 cm^{-1} has been attributed to the bended modes of O–C–H, C–C–H, and C–O–H [18]. A characteristic peak at 1640 cm^{-1} is apparently a feature of tightly bound water present in the starch [19]. In the spectrum of native starch, the peak at 2926 cm^{-1} corresponds to C–H stretching. An extremely broad band due to hydrogen bonded hydroxyl groups (O–H) appeared at 3400 cm^{-1} which was referred to the complex vibration stretches associated with free, inter and intra-molecular bound hydroxyl groups which make up the gross structure of starch. These FTIR bands support the presence of starch as well as glycosidic bonds in BRE. Spectrum of HEMA shows all its characteristic peaks. In case of BRE with HEMA disappearance of bands at 1634 cm^{-1}

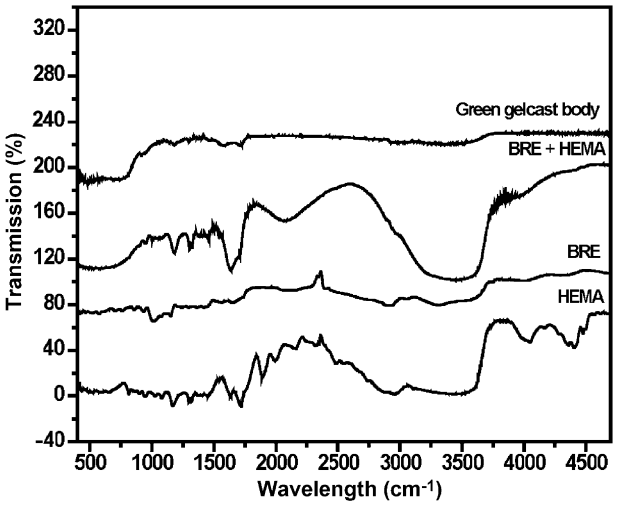

Fig. 3. FTIR spectra for HEMA, BRE powder, HEMA modified BRE and gelcast green body.

and 1718 cm^{-1} and simultaneous generation of broad single band at ~1600–1725 cm^{-1} and l920–2250 cm^{-1} range indicate some modification has taken place which leads to better stability of BRE after modification. Disappearance of band at ~1083 cm^{-1} indicates some modification of glycosidic linkage. Details investigation is under progress. Spectrum of green body shows presence of organic specimens. Dominant peaks centred at ~458 cm^{-1}, 604 cm^{-1} and 650 cm^{-1} are the characteristic peaks of the TiO_2.

3.3. X-ray diffraction (XRD) study

It has been observed in XRD studies that pure BRE became amorphous on heating above 80 °C. The gelatinization of BRE disrupted the crystalline structure. However, the modified BRE with 50% HEMA appeared crystallized even on heating beyond 80 °C. The modified starch granules start swelling above 60 °C and exist up to 120 °C.

3.4. Thermal analysis

In thermal studies the gelatinization phenomena of modified BRE with HEMA is confirmed in absence of negligible weight loss up to 120 °C heating with endothermic hump. DTA plot as depicted in Fig. 4a showed that unmodified BRE presents an endothermic peak between 275 °C and 300 °C, corresponding to the initiation of thermal decomposition whereas the degradation commences at 290–305 °C for modified BRE. However, the importance of amylose in phase transition associated to structural changes in starch granules in the amorphous regions are yet to confirm with detailed thermal studies.

The comparative DTA curve for BRE, base TiO_2 powder and TiO_2 green gelcast part [with 6 weight% binder to the total solid loading of 80% by weight] is shown in Fig. 4a. Many noticeable zones are observed for DTA curve of BRE. Endothermic peak ranging from 55 °C to 100 °C is assigned to BRE gelatinization [20] and the peak in the range of 110–125 °C can be attributed to the non-equilibrium melting of the complexes due to the partial recrystallization of amylose [21] and evaporation of loosely bound water. The endothermic peak in the range of 280-330 °C can be related to the depolymerization and degradation of amylose and amylopectin specimens in a non-oxidative process as well as internal water evaporation. Significant broad endothermic peak around 475–650 °C is attributed to the thermal degradation of BRE in presence of N_2 atmosphere. Broad humps in the range of 725–900 °C and 1050–1250 °C may be ascribed to the total degradation of intermediate products. In green gelcast part, the endothermic peak at 220–260 °C may be associated with early depolymerization and degradation of amylose and amylopectin specimens in a non-oxidative process. Further investigation on molecular conformation and structural determination is needed. Broad peak in DTA curve for TiO_2 powder and green compacts in the higher temperature range may be due to the phase transition from anatase to rutile TiO_2.

Thermo physical parameter plays an important role on thermal stability of BRE. Fig. 4b shows the major two stage mass loss up to 500 °C in the range of 0–10 weight% BRE content. The first minor one corresponds to the loss of adsorbed water and intermolecular water in the temperature range of 30–250 °C. The major mass loss corresponds to the starch materials decomposition in BRE in the temperature range of 250–475 °C. TG curve for green compacts with increasing binder content is shown in Fig. 4b. A total mass loss of 3.96–10.38% has been obtained for green gel-cast part with 2–10 weight% binder content. Total mass loss for green gelcast part of 80 weight% solid loading of TiO_2 with 6 weight% BRE is 7.37% where major mass loss approximately 5.0–5.2% corresponds to BRE powder.

3.5. Effect of ceramic processing parameters and modified BRE on gelcasting

3.5.1. Effects of BRE and dispersant concentration on zeta potential of the suspension

The effect of BRE on zeta potential has been studied. Inset in Fig. 5a shows the zeta potential of slurry as a function of BRE

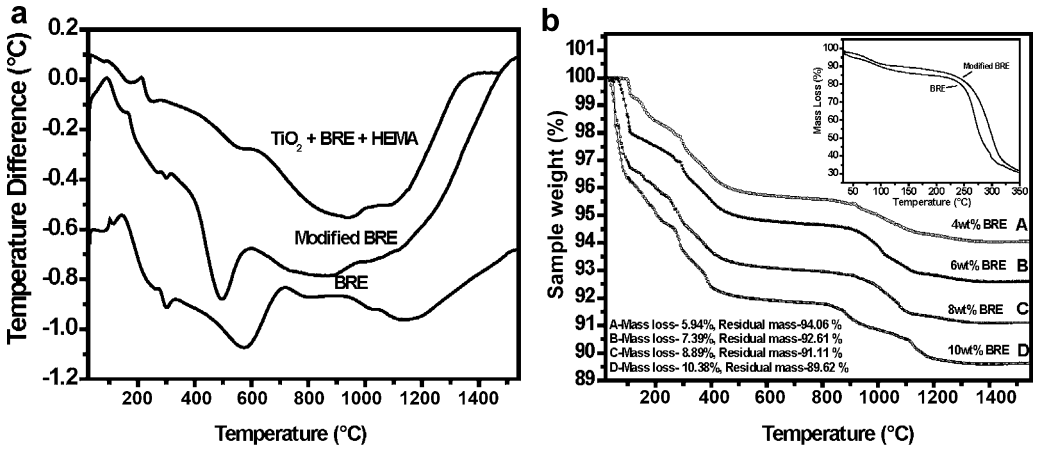

Fig. 4. (a): DTA curve for BRE, HEMA modified BRE and TiO_2 green body with BRE and HEMA. (b) TG mass loss for green compacts with different binder content. Inset: TG plot for native BRE and modified BRE.

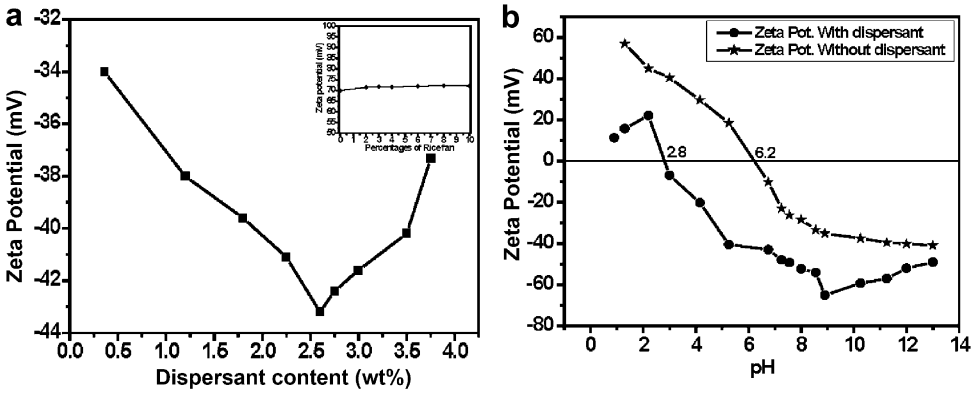

Fig. 5. (a): The influence of dispersant concentration on zeta potential of TiO_2 suspension. (b) Variation of Zeta potential with pH of the suspension in presence and absence of dispersant.

concentration. BRE used as a binder in the experiment is a starch with a large molecular structure does not affect zeta potential of the slurry. In gel casting system, it is needed to optimize the process parameters like dispersant amount and pH of the suspension for obtaining stable slurry with high concentration of solid particles. During suspension processing of titania slurry, the surface charge of the powder has a crucial effect on the state of particulate dispersion in presence of dispersants [22–24]. The surface electrical properties vis-à-vis polyelectrolyte concentration has been extensively studied with model polymer colloids by different researchers [25–27]. Darvan 821A (ammonium salt of polyacrylic acid, NH_4PAA) which was used as a dispersant in this study is a surface modifying agent. It helps to obtain colloidal-stable homogeneous slurry by reducing the inter-particle attraction forces between titania nanoparticles. The specific adsorption of the acrylate group on the titania surface leads to a higher charge density on the particle surface resulting in low enough viscosity suitable for gel casting. Dispersion stability of TiO_2 suspension is governed by the value of zeta potential [28]. The effect of the dispersant concentration on the zeta potential of TiO_2 powder is shown in Fig. 5a. Surface charge properties of titanium dioxide powder in aqueous suspensions were determined in terms of zeta potential using an electrophoresis technique. It can be observed that with an increase in dispersant concentration, the powder surface charge shows a sharp increase in the absolute value of zeta potential. Maximum zeta potential was obtained with highest fluidity when dispersant concentration was 2.6 weight% (with respect to the base nanopowder) in case of 80 weight% solid loaded slurry. However, when the dispersant concentration is beyond 2.6 weight%, the electrolyte causes charge reversal of the powder surface due to excessive adsorption of NH_4^+ ion and the positive zeta potential is too small to stabilize the powder. Further additions of NH_4PAA fail to be adsorbed on the surface and therefore the high electrolyte content in the suspension causes compression of the double layer.

A zero zeta potential is defined as iso-electric point (I.E.P) which is the indicative of uncharged (electrical neutrality) particle surface. This type of balancing of positive and negative charges leads to the flocculation of particles in suspension. With the addition of NH_4PAA as a dispersant the isoelectric point of nanosized TiO_2 particles shifts from pH 6.2 to pH 2.8. It was found that NH_4PAA adsorbs not only on charged TiO_2 but also beyond its point of zero charge [29]. A quantitative study was performed of polymeric dispersant adsorption on TiO_2 powders [30]. The electrokinetic's characterization and colloidal stability of different TiO_2/water interfaces under the presence of several electrolytes was studied [31].

3.5.2. *Effects of pH on zeta potential of the suspension*

The adsorption of NH_4PAA in the solid–solution interface depends on pH as it affects the degree of dissociation of the polymer. Fig. 5b shows the variation of zeta potential with pH of the slurry with or without the presence of dispersant. At higher pH, far from IEP, the titania particles have a high negative zeta potential and large colloidal stability. In aqueous systems, the dissociation behaviour of polyelectrolyte and the total charge of the polymer are pH dependent. At low pH values, the dissociated content of COOH-groups decreases, resulting in low surface charge of the polymer. In contrast at high pH values, the fraction of dissociated NH_4PAA increases and the polymer is essentially charged. Due to large possibility of agglomeration, slurries are unstable at the vicinity of isoelectric point and consist of large agglomerates which lead to porous gel cast ceramics. Fig. 5b shows that in presence of a dispersant, zeta potential is maximized at pH 8.9, which may provide better colloidal stability. The stability of slurry decreases at pH value higher than 9. This may be due to the decrease in ionization of NH_4PAA and maximum adsorption of dispersant on the powder surface.

3.5.3. *Effect of solid loading on slurry rheology*

One of the key issues in gelcasting is the production of a suspension with suitable quantity of binder. Rheological behaviour of slurries with different binder content is important to investigate. Optimization of appropriate amount of binder in preparation of ceramic slurry has an important role on the quality of ultimate products. The higher the binder content, the higher the viscosity of the slurry which in fact will lead to a

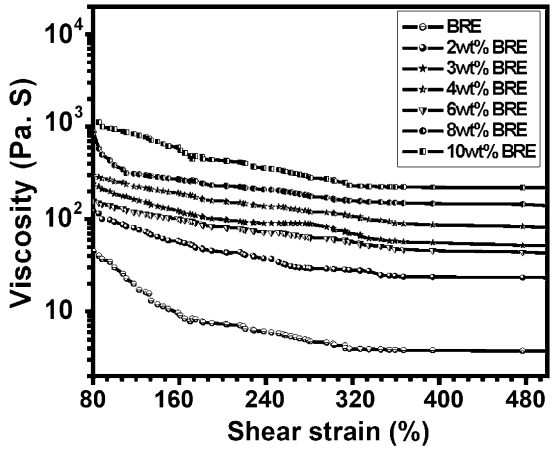

Fig. 6. Variation of viscosity with shear strain (%) for suspension with different binder concentrations.

green body of higher packing factor or higher density, thus minimizing the shrinkage of green body. But very high binder content makes the slurry inhomogeneous and highly viscous, difficult to cast. Suspension with acceptable amount of binder content must maintain its stability, homogeneity and fluidity with adequate viscosity for easy casting. The effect of binder content on slurry rheology for 80 weight% slurry is shown in Fig. 6. It can be seen that though all the suspensions exhibited a shear-thinning behaviour, only up to a reasonable amount of binder content slurry is homogeneous and viscosity is relatively low, which is suitable for casting. However, high binder content results in highly viscous and inhomogeneous suspension not suitable for gelcasting. This study has been carried out with 6 weight% of optimum binder content.

The rheological behaviour of slurries with high solid loading tends to be non-Newtonian. The higher the solid loading, the lower is the liquid content of the slurry in fact increases packing factor and density of green body. This also minimizes the shrinkage of the green body. The effects of solid loading content on rheology of slurry are shown in Fig. 7. In the present investigation, optimization of rheological properties by measuring viscosity of high concentrated suspensions

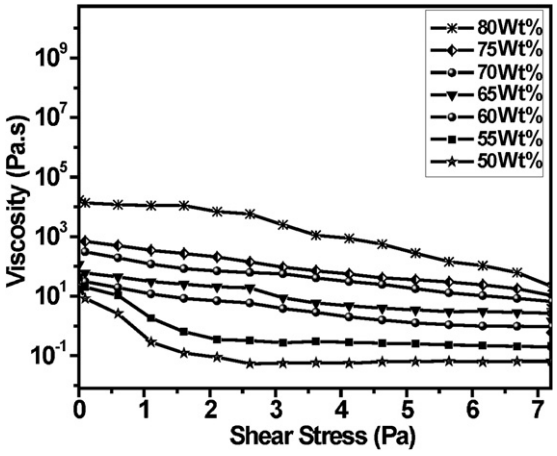

Fig. 7. Viscosity variation with stress for different solid loaded suspension.

containing nanometer-sized commercial titania powder has been done. Fig. 7 shows the plots of applied viscosity with shear stress of stable suspensions with different solid loading at 25 °C through viscometry measurement. With increasing solid loading viscosity increases as a result of increase in powder-to-liquid ratio leading to the decreasing distance among the powder particles. It is also seen that all suspensions with solid loading (50–80) weight% exhibit a shear-thinning behaviour and relatively low viscosity, making it suitable for gel casting. Fig. 8 shows flow curve of different solid loaded TiO_2 suspension. To investigate the rheological behaviour of TiO_2 slurry shear stress vs. shear rate relationship were fitted to pseudoplastic power law model, which is given by:

$$\iota = K\gamma^n \quad (1)$$

ι = Shear stress, K = fluid consistency index, γ = Shear rate, and n = flow behaviour index.

Fluid consistency index and flow behaviour index values at different shear rates calculated from power law model are shown as inset in Fig. 8.

3.6. Sintering and microstructure evaluation

The molecular conformation and structural determination as well as the effect of comparative gelation of modified glycoasidic linkages with HEMA are still under investigation with NMR and DSC studies respectively. Modification of BRE has been further evidenced from FESEM observation where fine starch granules are compared to the native starch as shown in Fig. 9a and b.

Microstructure uniformity of gel cast specimen is shown in Fig. 9. A FESEM photograph for green sample with 50k magnification is shown in Fig. 9c. Polished top surface image for sintered sample is shown in Fig. 9d. Fracture surfaces of the sintered body are depicted in Fig. 9e and f. From FESEM

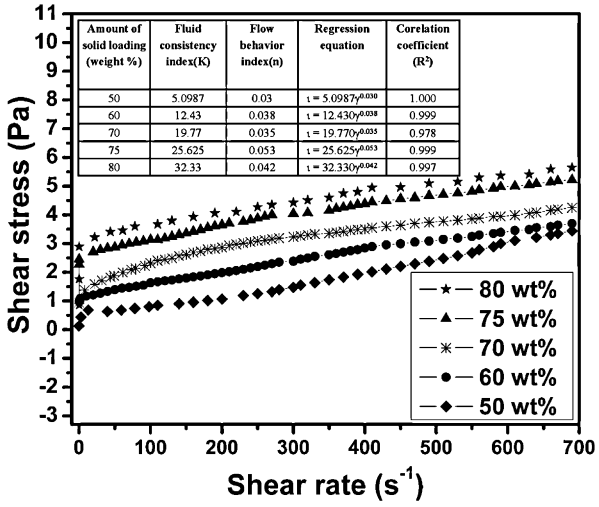

Fig. 8. Shear stress vs. shear rate curve for different solid loaded TiO_2 suspensions. Inset table shows rheological index values obtained from regression fitting of stress (ι) and strain (γ) in power law model.

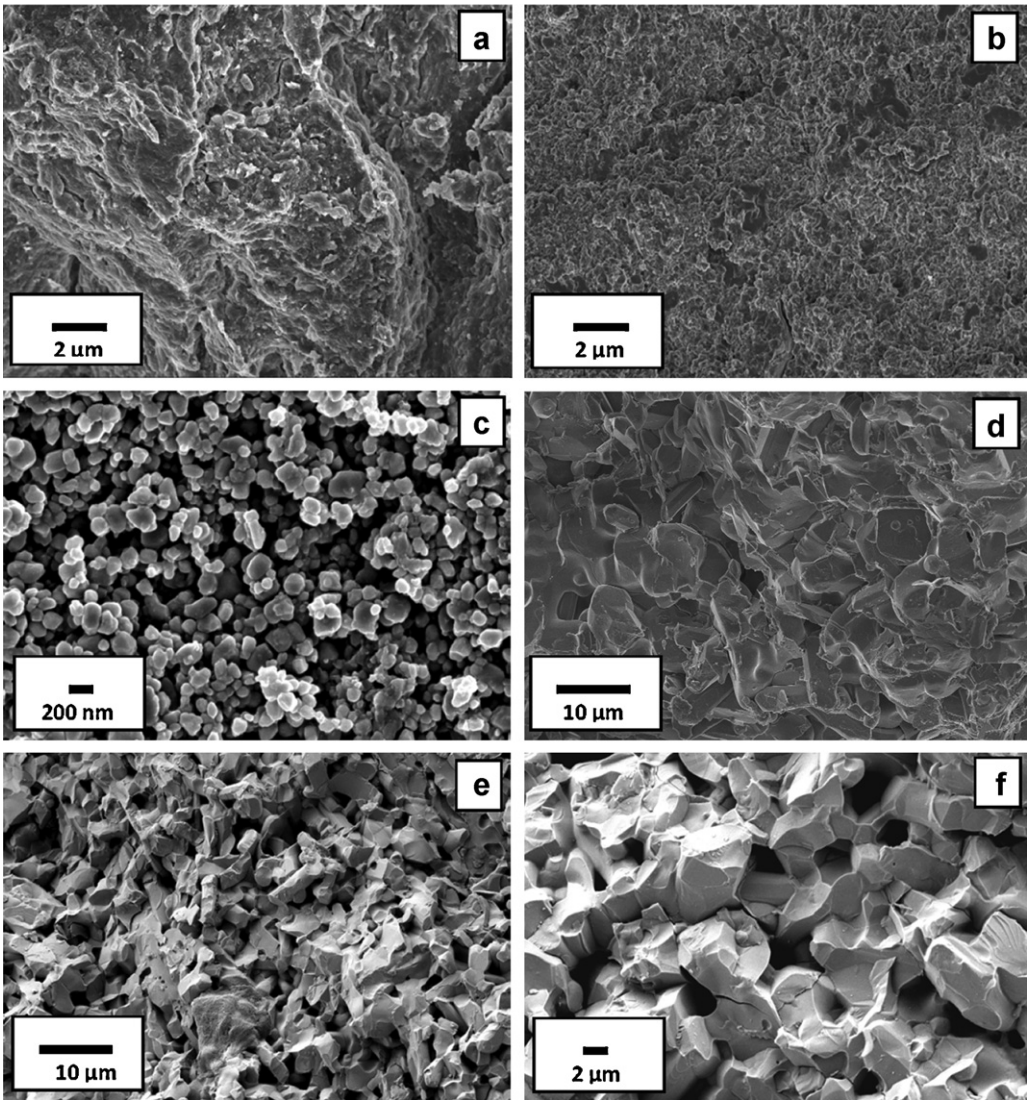

Fig. 9. (a): FESEM image of native BRE granules. (b) FESEM image of HEMA modified BRE granules. (c) Top surface FESEM micrographs of gelcast green body. (d) Top surface FESEM micrographs of gelcast sintered body. (e) Fracture surface FESEM micrographs of gelcast sintered body. (f) Fracture surface FESEM micrographs of gelcast sintered body at higher magnification.

Table 1
Different Shrinkage of gelcast TiO_2 bodies after drying and sintering.

Solid loading (weight%)	Volume shrinkage (%)		Linear shrinkage (%)					
			Length (%)		Width (%)		Height (%)	
	Drying (green)	Sintering at 1450 °C	Drying (green)	Sintering at 1450 °C	Drying (green)	Sintering at 1450 °C	Drying (green)	Sintering at 1450 °C
50	24.9	39.4	4.9	9.7	7.5	12.4	13.6	23.3
55	20.9	37.3	3.4	8.3	7.4	10.9	11.5	21.6
60	18.8	30.6	3.3	7.8	7.3	9.6	9.3	16.7
65	17.5	25.6	3.1	6.0	7.2	8.5	8.2	13.4
70	17.5	21.7	3.6	4.5	7.1	7.6	7.9	11.2
75	16.2	17.6	2.8	3.1	7.1	5.8	7.0	9.6
80	15.7	14.2	2.9	3.0	7.0	3.9	6.7	7.9

Fig. 10. Photographs of Titania gelcast components.

micrographs it can be seen that both green and sintered samples exhibit homogeneous microstructure with certain extent of pores.

3.7. Percent shrinkage and density study

Different linear (e.g., length, width and height) and volume shrinkages have been measured for green as well as sintered bodies. Table 1 indicates the comparative drying and sintering shrinkages (volume and linear shrinkage) for samples obtained from different solid loaded slurries. It can be seen that linear shrinkage as well as volume shrinkage decrease with increase in solid loading percentage as expected. Volume shrinkage on sintering for sample obtained from 50 weight% solid loaded suspension is as high as 39.38% compared to 24.95% in case of drying. Volume shrinkage for 80 weight% sintered sample is about 14.20%. Densities of sintered and green specimens were calculated from Archimedes principle (bulk density). Density for green as well as sintered samples obtained from different solid loaded slurry is shown in Table 2. The results show that the green densities as well as sintered densities increase with increase in solid loading resulting in minimizing the shrinkage of the body. As high as 96% of theoretical density has been achieved for 80 weight% solid loaded sintered sample. Photographs of some titania gel cast bodies are shown in Fig. 10.

Table 2
Density of gel cast TiO_2 bodies in the green and sintered state.

Solid content (weight%) in slurry	Density (g/cm^3)			
	Green density	% Theoretical density	Sintered	% Theoretical density
50	2.21	56.8	3.66	87
55	2.67	68.6	3.78	89
60	2.71	69.6	3.80	89
65	2.73	65.6	3.82	91
70	2.78	71.4	3.83	91
75	2.80	71.9	3.85	94
80	2.83	72.7	3.88	96

4. Conclusions

A gelcasting process involving boiling rice (BRE) extract modified with 2-hydroxyethylmethacrylate (HEMA) has been investigated leading to homogeneous titania slurry for gelcasting application. Swelling of modified starch creates an extruding force between TiO_2 particles and consolidates them. With gelatinization starch molecular chains extend to a great extent and create macromolecular network to hold the TiO_2 particles together. The iso-electrical point for this system shifts to a more acidic condition near pH 2.8 with the addition of NH_4PAA dispersant compared to pH 6.2 in de-ionized water without a dispersant. An optimum dispersant concentration is found to be 2.6 weight% at pH 8.9. Total mass loss for green compacts with 2–10 weight% binder content is around 3.96% to 10.38%. The TiO_2 ceramics with the homogeneous microstructure and the higher density (96%) has been made via the modified-starch consolidation process

using 6.0 weight% of a modified starch as a consolidator (network-former)/binder and sintering samples at 1450 °C for 1 h. BRE gelcasting system may be a valuable alternative to that based on a neurotoxic system.

Acknowledgements

The authors would like to express their gratitude to Prof. Gautam Biswas, Director, CSIR-CMERI for his kind permission to publish the paper. The authors are also grateful to Dept. of Science and Technology, Govt. of India for the financial support. The help rendered by our scientific & technical staffs of CAMP section, CMERI, Durgapur is acknowledged. The authors are also thankful to Mr. A. Paria and Mr. B. Das of IIT, Kharagpur for SEM and XRD analysis.

References

[1] O.O. Omatete, M.A. Janney, R.A. Strehlow, Gelcasting – a new ceramic forming process, Am. Ceram. Soc. Bull. 70 (1991) 1641–1647.
[2] O.O. Omatete, M.A. Janney, S.D. Nunn, Gelcasting: from laboratory development toward industrial production, J. Eur. Ceram. Soc. 17 (2-3) (1997) 407–413.
[3] L. Bergstrom, C.H. Schilling, I.A. Aksay, Consolidation behaviour of flocculated alumina suspension, J. Am. Ceram. Soc. 75 (12) (1992) 3305–3314.
[4] G.V. Franks, B.V. Velamakanni, F.F. Lange, Vibraforming and in situ flocculation of consolidated coagulated alumina slurries, J. Am. Ceram. Soc. 78 (5) (1995) 1324–1328.
[5] Y.L. Chen, Z.P. Xie, J.L. Yang, Y. Huang, Alumina casting based on gelation of gelatine, J. Eur. Ceram. Soc. 19 (2) (1999) 271–275.
[6] S.M. Olhero, G. Tarì, M.A. Coimbra, J.M.F. Ferreira, Synergy of polysaccharide mixtures in gelcasting of alumina, J. Eur. Ceram. Soc. 20 (4) (2000) 423–429.
[7] Y. Li, Z. Guo, J. Hao, S. Ren, Gelcasting of metal powders in non-toxic cellulose ether system, J. Mater. Process. Technol. 208 (1–3) (2008) 457–462.
[8] O. Lyckfeldt, J.M.F. Ferreira, Processing of porous ceramics by starch consolidation, J. Eur. Ceram. Soc. 18 (2) (1998) 131–140.
[9] A.J. Millán, R. Moreno, M.I. Nieto, Improved consolidation of alumina by agarose gelation, J. Eur. Ceram. Soc. 20 (14–15) (2000) 2527–2533.
[10] A.J. Millán, M.I. Nieto, R. Moreno, Near-net shaping of aqueous alumina slurries using carrageenans, J. Eur. Ceram. Soc. 22 (3) (2002) 297–303.
[11] L. Chen, X. Peng, Y. Huang, L. Li, X. Li, Controlling porosity and pore size distribution of alumina ceramics in consolidation forming process using modified starches, Key Eng. Mater. 368–372 (2008) 697–700.
[12] M. Huang, J.F. Kennedy, B. Li, X. Xu, B.J. Xie, Characters of rice starch gel modified by gellan, carrageenan and glucomannan: a texture profile analysis study, Carbohydr. Polym. 69 (2007) 411–418.
[13] J.U. Chenhui, W. Yanmin, Y. Jiandong, H. Yun, Modified-starch consolidation of alumina ceramics, J. Wuhan Univ. Technol.: Mater. Sci. Ed. 23 (4) (2008) 558–561.
[14] Z. Zivcová, E. Gregorová, W. Pabst, Low- and high-temperature processes and mechanisms in the preparation of porous ceramics via starch consolidation casting, Starch/Stärke 62 (2010) 3–10.
[15] R. Hoover, W.S. Ratnayake, Current Protocols in Food Analytical Chemistry, 2001, pp. E2.3.1–E2.3.5.
[16] H. Fehling, Die quantitative bestimmung von zucker und stärkmehl mittelst kupfervitriol, Justus Liebigs Annalen der Chemie 72 (1) (1849) 106–113.
[17] M. Marcazzan, F. Vianello, M. Scarpa, A. Rigo, An ESR assay for α-amylase activity toward succinylated starch, amylose and amylopectin, J. Biochem. Biophys. Methods 38 (1999) 191–202.
[18] V.B. Maurel, C. Vallat, D. Goffinet, Quantitative analysis of individual sugars during starch hydrolysis by FT-IR/ATR spectrometry. Part II: influence of external factors and wavelength parameters, Appl. Spectrosc. 49 (5) (1995) 563–568.
[19] M. Kacurakova, R.H. Wilson, Developments in mid-infrared FT-IR spectroscopy of selected carbohydrates, Carbohydr. Polym. 44 (2001) 291–303.
[20] L. Zhiqiang, Y.S. Xiao, F. Yi, Effect of bound water on thermal behaviours of native starch, amylose and amylopectin, Starch-Stärke 51 (11–12) (2000) 406–410.
[21] L.S. Guinesi, A.L. da Róz, E. Corradini, L.H.C. Mattoso, E.d.M. Teixeira, A.A.d.S. Curvelo, Kinetics of thermal degradation applied to starches from different botanical origins by non-isothermal procedures, Thermochim. Acta 447 (2) (2006) 190–196.
[22] M.R.B. Romdhane, T. Chartier, S. Baklouti, J. Bouaziz, C. Pagnoux, J.F. Baumard, A new processing aid for dry pressing: a copolymer acting as dispersant and binder, J. Eur. Ceram. Soc. 27 (7) (2007) 2687–2695.
[23] K. Cai, M. Ode, H. Murakami, Influence of aqueous polyelectrolyte dispersants on the surface chemical properties of aluminum in suspension, Colloid Surf. A: Physicochem. Eng. Aspect 284–285 (2006) 458–463.
[24] B.P. Singh, S. Bhattacharjee, L. Besra, D.K. Sengupta, Electrokinetic and adsorption studies of alumina suspensions using Darvan C as dispersant, J. Colloid Interface Sci. 289 (2) (2005) 592–596.
[25] J.M. Peula-García, R. Hidalgo-Alvarez, F.J. de las Nieves, Colloid stability and electrokinetic characterization of polymer colloids prepared by different methods, Colloid Surf. A 127 (1–3) (1997) 19–24.
[26] B.R. Midmore, G.V. Pratt, T.M. Herrington, Evidence for the validity of electrokinetic theory in the thin double layer region, J. Colloid Interface Sci. 184 (1) (1996) 170–174.
[27] G. Girod, J.M. Lamarche, A. Foissy, Adsorption of partially hydrolyzed polyacrylamides on titanium dioxide, J. Colloid Interface Sci. 121 (1) (1988) 265–272.
[28] R. Greenwood, Review of the measurement of zeta potentials in concentrated aqueous suspensions using electroacoustics, Adv. Colloid Interface Sci. 106 (1–3) (2003) 55–81.
[29] A. Foissy, A. El Attar, J.M. Lamarche, Adsorption of polyacrylic acid on titanium dioxide, J. Colloid Interface Sci. 96 (1) (1983) 275–287.
[30] M.A. Banash, S.G. Croll, A quantitative study of polymeric dispersant adsorption onto oxide-coated titania pigments, Prog. Org. Coat. 35 (1–4) (1999) 37–44.
[31] A. Fernández-Nieves, F.J. de las Nieves, The role of ζ potential in the colloidal stability of different TiO_2/electrolyte solution interfaces, Colloid Surf. A 148 (3) (1999) 231–243.